International Journal of Materials and Chemistry 2025, 15(3): 54-58
DOI: 10.5923/j.ijmc.20251503.05

Morphology, Structure, and Electrical Conductivity of Cellulose–Polythiophene Composite: Hierarchical Organization and Synergistic Effects

Galia Zhunsalieva[1,*], Nuritdin Kattaev[2], Khamdam Akbarov[2]

[1]PhD Student, Department of Physical Chemistry, National University of Uzbekistan, Tashkent, Uzbekistan
[2]DSc, Professor, Department of Physical Chemistry, National University of Uzbekistan, Tashkent, Uzbekistan

Abstract This work presents the results of a comprehensive study of a cellulose–polythiophene composite synthesized by oxidative polymerization of thiophene on the surface of a biopolymer matrix. Scanning electron microscopy revealed a sponge-like nanogranular structure of polythiophene with particle sizes of 10–100 nm and a developed porosity (~53%), as well as the fibrillar morphology of cellulose partially coated with the polymer (~21% of the surface). X-ray diffraction analysis demonstrated a hybrid amorphous–crystalline structure: low-angle diffuse maxima correspond to the cellulose matrix, while sharp peaks in the range of 37–65° 2θ are associated with crystalline domains of polythiophene with an average size of ~45 nm (calculated using the Scherrer equation). Thermogravimetric analysis confirmed the multistage character of thermal decomposition, with the composite exhibiting intermediate but improved thermal stability compared to pure cellulose. Current–voltage characteristics showed a linear and symmetric profile and an increase in specific conductivity by more than three orders of magnitude (from $2.4 \cdot 10^{-11}$ to $7.2 \cdot 10^{-10}$ S/m) with increased polymerization time. It is established that the cellulose–polythiophene system possesses a hierarchical morphology and synergistic properties: mechanical flexibility and biocompatibility from cellulose, combined with the electrical conductivity and thermal stability of polythiophene. The composite is considered a promising material for applications in supercapacitors, sensors, membrane technologies, and flexible electronics.

Keywords Cellulose, Polythiophene, Composite, Electrical conductivity, Nanostructure

1. Introduction

Modern trends in materials science are focused on the creation of functional composites that combine the properties of organic and inorganic components. Particular attention is paid to conducting polymers, which, due to the presence of π-conjugated systems, can ensure efficient charge transport and are applied in electrochemical devices, sensors, supercapacitors, and flexible electronics [1-3]. Among such materials, polythiophene and its derivatives (e.g., PEDOT) occupy a key position due to their high chemical stability, tunable conductivity, and compatibility with different matrices [4,5].

At the same time, the use of biopolymers as matrices for conducting materials not only reduces cost and environmental impact but also imparts new functional characteristics. Cellulose is the most abundant natural polymer, combining mechanical strength, biocompatibility, and availability. Its fibrillar structure, developed surface, and the presence of hydroxyl groups create favorable conditions for the deposition and anchoring of conducting polymers [6-8].

The development of cellulose–polythiophene composites offers great potential for new functional materials. Such composites combine the flexibility and biocompatibility of cellulose with the conductivity and electrochemical activity of polythiophene. However, the efficiency of these systems is largely determined by their morphology, degree of crystallinity, thermal stability, and the distribution of the conducting phase in the matrix. Therefore, the aim of this work was the synthesis and comprehensive investigation of the cellulose–polythiophene composite, focusing on morphology, structural characteristics, thermal stability, and electrical properties.

2. Materials and Methods

Reagents.

- Thiophene (C_4H_4S, analytical grade) – used as the monomer for polymerization.

* Corresponding author:
g.junsalieva@gmail.com (Galia Zhunsalieva)
Received: Sep. 11, 2025; Accepted: Sep. 27, 2025; Published: Sep. 29, 2025
Published online at http://journal.sapub.org/ijmc

- Ferric chloride ($FeCl_3$, anhydrous) – used as the oxidizing agent for polythiophene and PT/S composites.
- Dichloromethane (CH_2Cl_2, analytical grade) – the main solvent for thiophene polymerization.
- Acetonitrile (CH_3CN, analytical grade) – used to dissolve $FeCl_3$.
- Acetone (CH_3COCH_3, analytical grade) – used for washing the polymer and composites.
- Distilled water – used for washing the samples.
- Microcrystalline cellulose – served as the matrix for forming cellulose–polythiophene composites.

All reagents were of analytical grade and used without further purification.

Synthesis of Polythiophene (PT).

Polythiophene was synthesized via the classical oxidative chemical polymerization method. Thiophene monomer (0.5 M) was dissolved in 100 mL of dichloromethane in a flat-bottom flask. Freshly prepared anhydrous $FeCl_3$ was dissolved in acetonitrile with vigorous stirring and added dropwise to the thiophene solution. The appearance of a dark-red, then black coloration indicated polymerization. The reaction proceeded under stirring for a fixed time. The resulting PT was filtered and repeatedly washed with acetone and acetonitrile until the filtrate became colorless, then dried in a vacuum oven at 60 ℃ for 24 h.

Synthesis of PT/S Composites.

Composite films were obtained by oxidative polymerization of thiophene in the presence of cellulose. As an oxidizing agent, $FeCl_3$ was used [9]. Dichloromethane was selected as the optimal solvent. In a typical experiment, 0.8 mL of thiophene was dissolved in 25 mL of dichloromethane. To initiate polymerization, a suspension of the oxidizer (0.025 mol of $FeCl_3$ dissolved in 25 mL of acetonitrile) was added dropwise under stirring. Reaction mixtures were stirred at room temperature for 4, 14, and 24 h, yielding PT/S-4, PT/S-14, and PT/S-24 samples, respectively. The color change from red to dark brown confirmed polymerization. Unreacted thiophene and $FeCl_3$ residues were removed by ultrasonic treatment for 5 min, followed by drying at room temperature for 24 h.

Characterization Methods.

- **SEM:** Morphology and coating distribution were examined at ×500 and ×10,000 magnifications. Porosity and particle size distributions were analyzed using image processing.
- **XRD:** X-ray diffraction patterns were recorded with Cu Kα radiation (λ = 1.5406 Å) in the 2θ range 5–70 °, at 40 kV and 30 mA. Crystallite sizes were calculated using the Scherrer equation.
- **TGA/DTA:** Thermal analysis was performed from 30 to 700 ℃ at a heating rate of 10 ℃/min in air, recording mass losses and decomposition stages.
- **Electrical measurements (I–V):** Current–voltage characteristics were measured up to 300 V. Specific conductivity was calculated using $\sigma = G \cdot L/A$, where G is conductance, L is the film thickness (~30 μm), and A is the contact area (1 cm^2).

3. Results and Discussion

Morphology (SEM).

SEM analysis revealed that pristine polythiophene (PT) exhibited a nanogranular sponge-like morphology with a highly porous architecture. At ×10,000 magnification (Fig. 1a), spherical and irregularly shaped grains ranging from 10 to 100 nm were observed (median ~21 nm, mean ~53 nm). The porous fraction accounted for ~53% of the surface, with pore sizes distributed from a few nanometers to several hundred nanometers (median ~19.5 nm). Such a combination of nanoscale particles and developed porosity results in a hierarchical structure that is advantageous for electrochemical processes, as it maximizes the accessible surface area and facilitates the penetration of electrolyte species. Additional image analysis confirmed a correlation length of ~0.15 μm and a fractal dimension of ~1.31, indicative of a network-like morphology capable of supporting percolative charge transport.

In cellulose–polythiophene composites (Fig. 1b, ×500), the fibrillar structure of cellulose was partially coated by PT, covering ~21% of the surface. The porous fraction increased to ~78%, with pore sizes spanning submicron to tens of microns (median ~1.8 μm, mean ~12 μm). This coexistence of micro- and mesoporosity ensures both efficient electrolyte diffusion and strong interfacial contact between the conducting polymer and the cellulose substrate. FFT analysis showed a pronounced anisotropy with a dominant orientation at ~91 °, coinciding with cellulose fiber alignment (anisotropy ratio ~5.45). The total groove length of ~6.3 mm in the field of view confirmed a well-developed relief providing additional "anchoring sites" for polymer adhesion [6–8].

Structure (XRD).

XRD confirmed the hybrid amorphous–crystalline nature of the composites. Diffuse low-angle maxima (10–15° 2θ, interplanar spacing 7–8 Å) reflected the semicrystalline nature of cellulose, while sharp peaks at 2θ = 37.5° (d = 2.39 Å), 43.8 ° (d = 2.07 Å), and 64.1 ° (d = 1.45 Å) indicated polythiophene crystalline domains (Fig.2). Crystallite sizes determined by the Scherrer equation were 42, 48, and 45 nm, with an average of ~45 nm, consistent with reported values for polythiophene and PEDOT (20–50 nm) [4,5,10]. In biopolymer-based composites, crystallite stabilization typically results in sizes up to 40–60 nm [12], in full agreement with our findings. These nanocrystalline domains are expected to enhance charge delocalization along π-conjugated backbones, contributing to improved electrical performance.

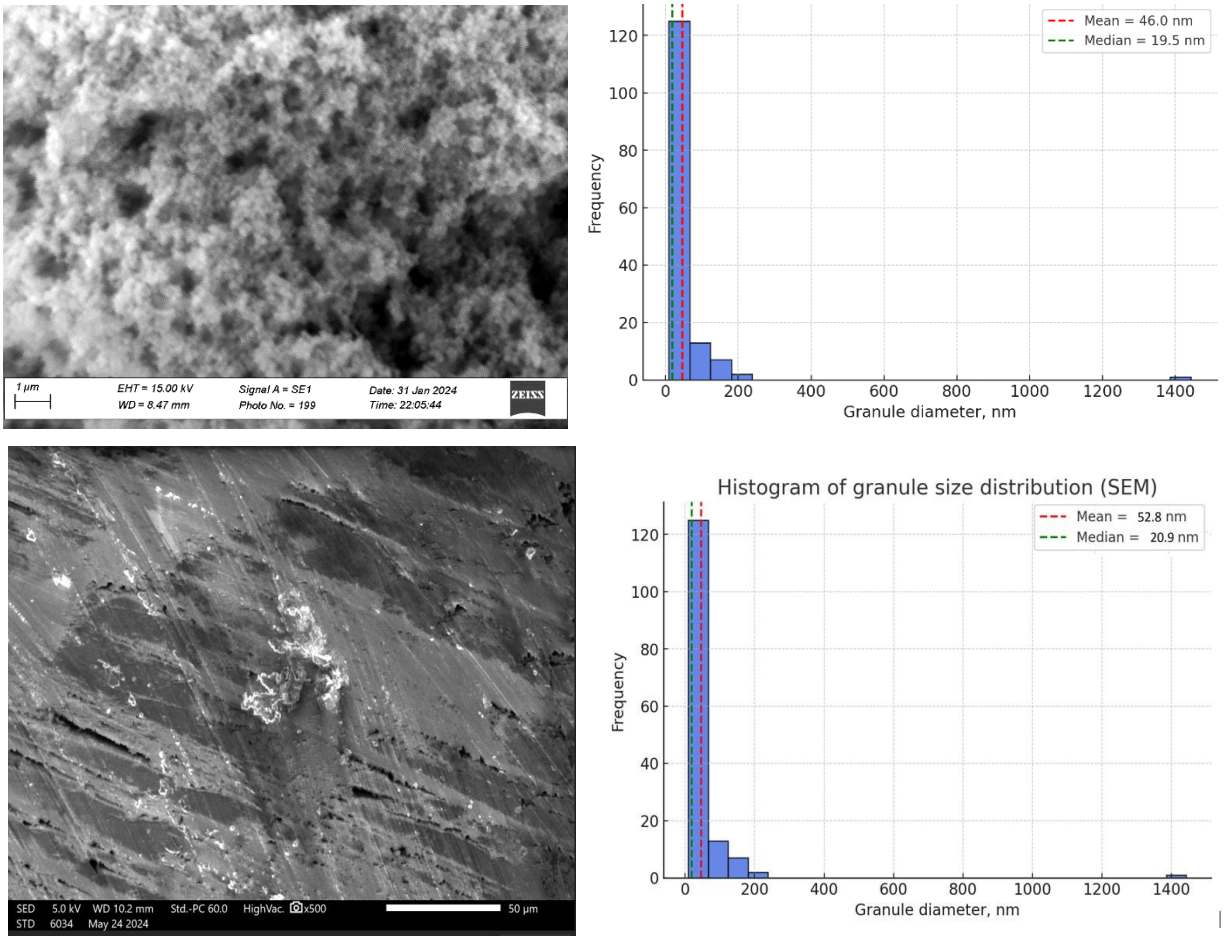

Figure 1. SEM micrographs of particle size distribution of polythiophene (a) and cellulose-polythiophene composite (b)

Thermal Stability (TGA/DTA).

Thermal analysis (Fig. 3) demonstrated a three-step decomposition pathway. The first stage (37–250 ℃, ~8.7% mass loss) corresponded to the removal of water and volatiles, extended compared to pure cellulose due to PT acting as a diffusion barrier. The second stage (250–500 ℃, ~64% mass loss) reflected the combined degradation of cellulose glycosidic bonds and PT conjugated chains. Notably, the onset temperature was shifted upward compared to neat cellulose (200–350 ℃), confirming a stabilizing effect from PT. The third stage (501–702 ℃, ~8.8% mass loss) corresponded to carbonization, yielding a residual carbonaceous fraction. This residue is characteristic of conducting polymers and supports enhanced thermal stability compared to pure cellulose, which typically leaves minimal residue in this region. The overall behavior thus represents intermediate but improved stability relative to the pristine components [11].

Electrical Conductivity (I–V).

The electrical behavior of cellulose–PT composites was studied as a function of polymerization time (4, 14, and 24 h). I–V curves for all samples were linear and symmetric (Fig. 4), confirming ohmic conduction without rectifying junctions or significant interfacial barriers. This indicates that current transport is governed by bulk percolation pathways rather than interfacial injection processes.

Quantitative analysis revealed a dramatic increase in conductance with polymerization time. For short polymerization (4 h), the current at ~250–300 V was ~20 nA, corresponding to a conductance of ~0.08 nS and a specific conductivity of $2.4 \cdot 10^{-11}$ S/m. For 14 h polymerization, the current increased to ~150 nA, conductance reached ~0.6 nS, and conductivity was $1.8 \cdot 10^{-10}$ S/m. Finally, after 24 h polymerization, the current rose to ~600 nA, conductance to ~2.4 nS, and conductivity to $7.2 \cdot 10^{-10}$ S/m. Overall, the specific conductivity increased by more than three orders of magnitude between short and long polymerization times.

This superlinear increase is a hallmark of percolation-driven conduction. At early stages, PT forms isolated clusters with poor interconnectivity, and current is limited to tunneling between localized islands. As polymerization progresses, the coverage of cellulose fibrils by PT increases, interparticle bridges form, and the system approaches the percolation threshold. Once this threshold is exceeded, a continuous PT network emerges, resulting in a steep rise in conductivity. Such behavior is consistent with percolation scaling laws, where conductivity follows $\sigma \propto (p - p\_c)\text{^}t$, with t typically between 1.6 and 3 for disordered systems [3,7].

Importantly, the linearity and symmetry of I–V curves at all synthesis durations suggest that conduction is not limited by electrode–film interfaces but rather by the connectivity of PT domains within the cellulose matrix. The absence of

hysteresis further supports a stable ohmic mechanism. Compared with literature values, pure cellulose is insulating (10^{-12}–10^{-14} S/cm), while undoped polythiophene exhibits conductivities of 10^{-6}–10^{-3} S/cm. PEDOT:PSS–cellulose composites have reached 10^{-2}–10^{-1} S/cm under optimized conditions [12]. Our results place the cellulose–PT system at an intermediate level: significantly enhanced conductivity compared to cellulose, tunable with polymerization time, but lower than PEDOT-based benchmarks. This highlights both the potential of the system and the importance of further optimization, for instance by enhancing doping levels or introducing co-polymers.

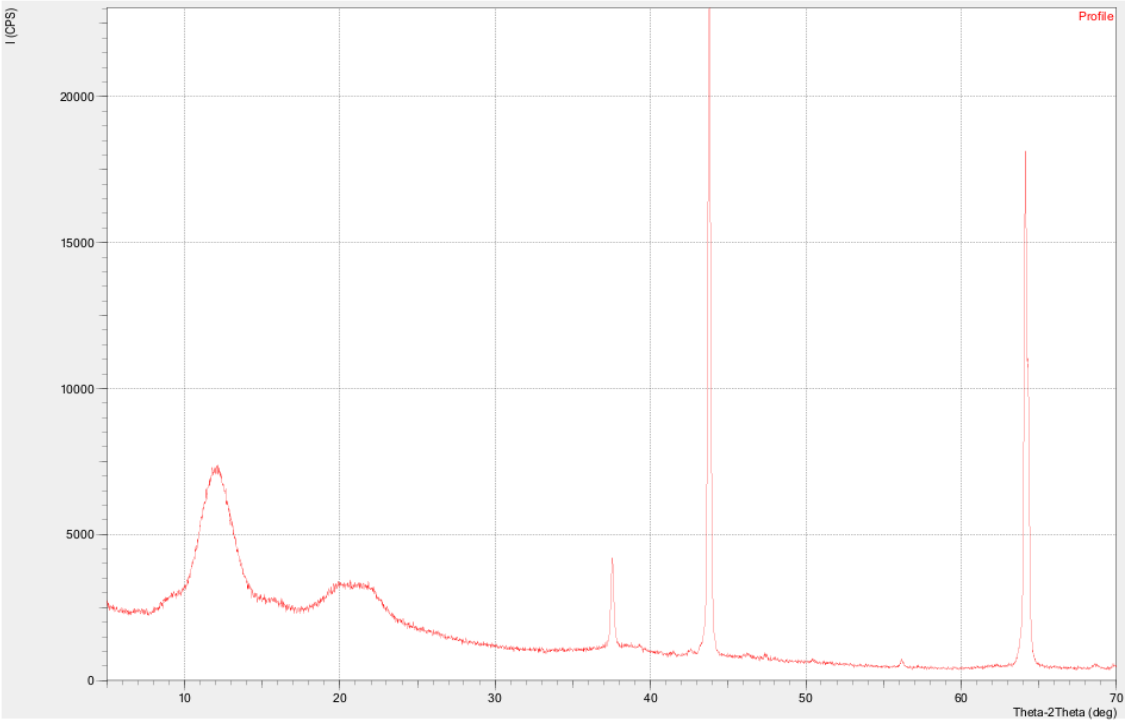

Figure 2. X-ray diffraction pattern of cellulose-polythiophene composite

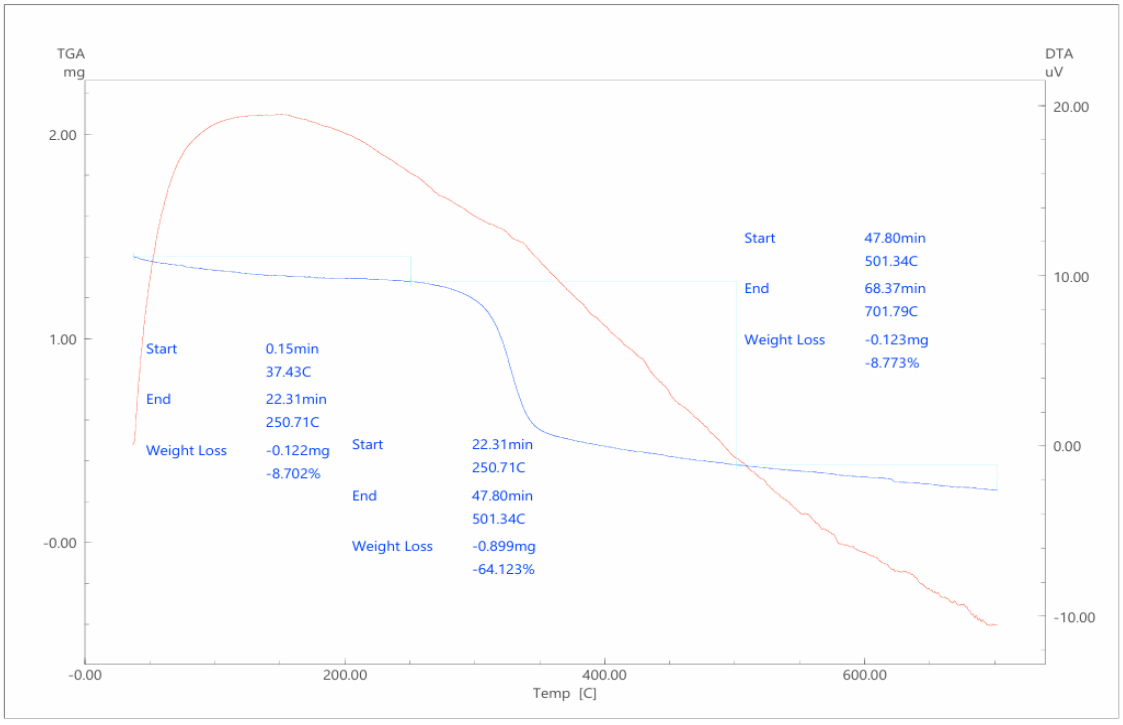

Figure 3. Derivatogram of a cellulose-polythiophene composite

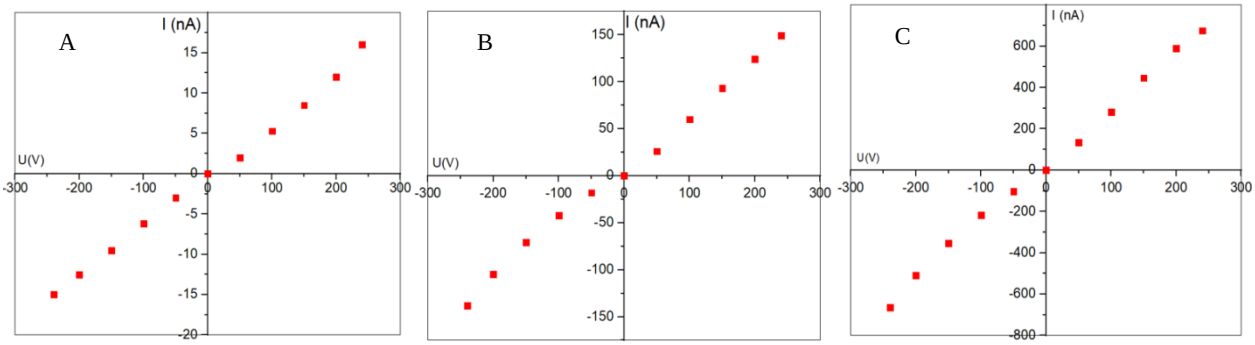

Figure 4. Forward and reverse current-voltage characteristics of the cellulose-polythiophene composite at different (4 (A), 14 (B) and 24 (C) hours) times of thiophene polymerization

The ability to tune conductivity over several orders of magnitude simply by controlling polymerization time underscores the versatility of this approach. From an application perspective, lower-conductivity membranes may be advantageous for ion-selective sensing, while higher-conductivity films could serve as current collectors or active layers in supercapacitors. Moreover, the structural anisotropy induced by the cellulose template may provide directionally dependent transport, useful in flexible electronics and membrane technologies.

4. Conclusions

The cellulose–polythiophene composite exhibits a hierarchical morphology with nanoscale PT crystallites (~45 nm), macroscopic cellulose orientation, high porosity, and structural anisotropy. These features provide a balance of mechanical flexibility, thermal stability, and tunable conductivity, making the composite a promising material for supercapacitors, sensors, membrane technologies, and flexible electronics.

REFERENCES

[1] Skotheim, T. A.; Reynolds, J. R. *Handbook of Conducting Polymers*; CRC Press: Boca Raton, 2007.

[2] Heinze, J.; Frontana-Uribe, B. A.; Ludwigs, S. Electrochemistry of Conducting Polymers–Persistent Models and New Concepts. *Chem. Rev.* 2010, *110*, 4724–4771. https://doi.org/10.1021/cr900226k.

[3] Bubnova, O.; Crispin, X. Towards Polymer-Based Organic Thermoelectric Generators. *Energy Environ. Sci.* 2012, *5*, 9345–9362. https://doi.org/10.1039/C2EE22777K.

[4] Roncali, J. Conjugated Poly(thiophenes): Synthesis, Functionalization, and Applications. *Chem. Rev.* 1997, *97*, 173–206. https://doi.org/10.1021/cr950257e.

[5] Zhang, X.; Yang, D.; Zhao, Y. Structure and Properties of PEDOT and Polythiophene Derivatives: A Review. *Synth. Met.* 2017, *225*, 13–30. https://doi.org/10.1016/j.synthmet.2016.12.018.

[6] Klemm, D.; Heublein, B.; Fink, H.-P.; Bohn, A. Cellulose: Fascinating Biopolymer and Sustainable Raw Material. *Angew. Chem. Int. Ed.* 2005, *44*, 3358–3393. https://doi.org/10.1002/anie.200460587.

[7] Isogai, A.; Saito, T.; Fukuzumi, H. TEMPO-Oxidized Cellulose Nanofibers. *Nanoscale* 2011, *3*, 71–85. https://doi.org/10.1039/C0NR00583E.

[8] Habibi, Y.; Lucia, L. A.; Rojas, O. J. Cellulose Nanocrystals: Chemistry, Self-Assembly, and Applications. *Chem. Rev.* 2010, *110*, 3479–3500. https://doi.org/10.1021/cr900339w.

[9] Groenendaal, L.; Zotti, G.; Aubert, P.-H.; Waybright, S. M.; Reynolds, J. R. Electrochemistry of Poly(3,4-ethylenedioxythiophene): The Most Studied Conducting Polymer. *Adv. Mater.* 2003, *15*, 855–879. https://doi.org/10.1002/adma.200300322.

[10] Park, S. H.; Roy, A.; Beaupré, S.; Cho, S.; Coates, N.; Moon, J. S.; Moses, D.; Leclerc, M.; Lee, K.; Heeger, A. J. Bulk Heterojunction Solar Cells with Internal Quantum Efficiency Approaching 100%. *Nat. Photonics* 2009, *3*, 297–302. https://doi.org/10.1038/nphoton.2009.69.

[11] Po, R.; Bernardi, A.; Calabrese, A.; Carbonera, C.; Corso, G.; Pellegrino, A. From Lab to Fab: How Must the Polymer Solar Cell Materials Design Change? *Energy Environ. Sci.* 2014, *7*, 925–943. https://doi.org/10.1039/C3EE43416A.

[12] Sajjadi, S. A.; Jahandideh, A.; Arjmand, M. Cellulose-Based Nanocomposites for Energy Storage Applications. *Carbohydr. Polym.* 2020, *250*, 116885. https://doi.org/10.1016/j.carbpol.2020.116885.